Optical Tweezers Microscopy: picoNewton forces in cell and molecular biology

Chapter 16 (Accepted Draft)

Book: NANOSCOPY and multidimensional optical fluorescence microscopy

Edited by Alberto Diaspro

Publisher: Chapman and Hall/CRC, 2010 ISBN: 9781420078862, 445 pages

Table of contents

Optical Tweezers Microscopy: picoNewton forces in cell and molecular biology

Difato F.[1], Ferrari E.[2], Shahapure R.[3], Torre V.[3,4] and Cojoc D[5].

1. Italian Institute of Technology, Genoa, Italy.
2. MRC Laboratory of Molecular Biology, Neurobiology Division, Cambridge, United Kingdom
3. International School for Advanced Studies (SISSA-ISAS), Trieste, Italy.
4. Italian Institute of Technology, ISAS Unit, Italy.
5. CNR-INFM Laboratorio Nazionale TASC, Trieste, Italy,

Introduction

Optical microscopes, from simple lens optical systems to advanced fluorescence instruments, played a fundamental role in medicine and biology as they permit observation of living systems in their native environment with a low level of structural and functional perturbation[1].
The spatial resolution in normal microscopes is diffraction limited to about 200 nm laterally and 500 nm axially but the size of the features of interest in cell biology (organelles, molecules, macromolecules) is much less[2]. Therefore, the enhancement of the spatial resolution represents a very important research issue for the worldwide scientists. The advent of viable physical concepts of overcoming the limiting role of diffraction in the last fifteen years set off a quest that has led to readily applicable and widely accessible fluorescence microscopes with nanoscale spatial resolution[3,4].
On the other hand, all living cells face mechanical forces which are converted into biochemical signals and integrated into the cellular responses (mechanotransduction). Therefore, the development of new techniques for exerting mechanical stresses on cells and observe their responses is crucial to clarify the molecule-and cell-level structures that may participate in mechanotransduction[5]. Forces can be exerted on a cell by a variety of experimental techniques. If the force is in the right range of magnitude it is capable of eliciting a biological response from the cell. For instance, in the case of fluid shear, the critical level of stress for a variety of biological responses has been observed to be of about 1 Pa. Integrated over the entire apical surface of a vascular endothelial cell (about 1,000 μm^2), this produces a total force of 1 nN. Other experiments with forces applied via tethered beads also exhibit a threshold value of about 1 nN. If the total applied force is balanced solely by the forces in focal adhesions that occupy only 1% of the basal surface area, then the stress on the focal adhesions amplifies 100-fold to 100 Pa. On the contrary, a stress of 1 Pa on a focal adhesion, which might activate a local biological response of the cell, requires applying a force of about 10 pN only. The level of force needed to produce significant conformational change in the force-transmitting proteins can also be estimated. The force that causes the bond between two proteins to rupture establishes an upper bound. Several studies have measured the fibronectin/integrin bond strength[6], producing estimates in the range of 30–100 pN. Forces as low as 3–5 pN have also been shown to be sufficient to unfold certain subdomains in fibronectin[7]. If external force is capable of producing a significant change in intracellular biochemical reaction rates, then the effect of force on protein conformation must exceed that associated with thermal fluctuations. Given that thermal energy, kT, is ~4 pN·nm, and considering conformational changes with a characteristic length scale of 1–10 nm, the corresponding force levels would fall in the range 0.4–4 pN[5]. This happens to coincide with the magnitude of force that can be produced by a

single myosin molecule[8], consistent with the theory that active cellular contraction can induce cell signalling. Therefore, all this would suggest that the critical values of force exerted on a single molecule fall within the pN range.

Interestingly to notice, this is also the range of forces exerted on the particle in an optical trap by the radiation pressure of light. This relatively young technique[9] provides the non-mechanical manipulation of the biological particles such as virus, living cells and subcellular organelles.

Optical Tweezers are now being used in the investigation of an increasing number of biochemical and biophysical processes, from the mechanical properties of biological polymers to the multitude of molecular machines that drive the internal dynamics of the cell[10].

It enable to control the spatial organization of samples: to perform sorting and/or to induce specific interactions between sample particles, at arbitrary location and time[11].

An optical trap can be also calibrated to perform force spectroscopy measurements. The optical tweezers system in this configuration is sometime called Photonic Force Microscope (PFM)[12].

The acronym PFM for photon force microscopy has been introduced in analogy with the Atomic Force Microscope. The probe, cantilever tip for the AFM, is replaced by the trapped bead in PFM. From the point of view of force measurement, the main difference between the AFM and PFM is the stiffness of the probe. The stiffness for an optically trapped probe is usually much lower (1-2 order of magnitudes) than the mechanical cantilever probe of the AFM. This makes the PFM complementary to AFM for force measurements in cell biology.

Optical tweezers microscopy is compatible with many fluorescence imaging techniques. Therefore it is possible to apply localized mechanical and chemical stimuli on cells while following changes in cell shape and organization[13].The combination of chemical and mechanical stimulation is useful and relevant in cell biology, since cells test the extracellular matrix rigidity during their differentiation[14] and they take up a polarized organization in culture dish which influences their structure and function (in fact tissue-specific architecture and cell–cell communication are lost on the 2D arrangement of the culture dish[15]). Many laboratories are now studying different types of 3D scaffolds to grow cell cultures in a three dimensional tissue-like fashion[16].

In this context, a better understanding of the mechanisms by which cells compute mechanical transductions during differentiation in tissue development is necessary, i.e. how contact inhibition regulates cell proliferation and how mechanical tensions regulate single cell and global tissue shape[17].

Since the late 19th century, Julius Wolff proposed the idea that bone is deposited and modelled in response to mechanical stress. Intrinsic mechanical properties of the cell microenvironment influence cell function both in vitro and in vivo, therefore Wolff's Law may be extended to the development of any kind of tissue throughout the body[14]. In the tensegrity model of Ingberg, the cellular organization is explained as a scaffold of tensed and compressed cables. The cytoskeleton, which defines the cell compartmentalization, and structure changes in the equilibrium of such cables influence the cell behavior[18]. It is known, for instance, that cells expand where extra-cellular matrix (ECM) is stiffer. To test the stiffness of the external environment, a cell performs contraction on its binding sites[19], which are clustered at special protruding structures[20].

The high sensitivity of PFM has permitted to measure forces in the piconewton range, which is relevant in cell biology: mechanical properties of cell membranes, DNA molecule, and

filamentous proteins have been quantified[21]. Force measurements represent an additional information in the multidimensional dataset which can be obtained using an optical microscope and, moreover, a new point of view in biology studies: it can be applied to understand how physical forces within the cell interact to form a stable architecture[22], how cells resist physical stresses, and how changes in the cytoskeleton initiate biochemical reactions.
In addition, PFM can help in explaining the mechanical rules that cause molecules to assemble.
An interesting example is the study of the shell of a virus, which consists of several subunits of proteins, to understand how it can self assemble starting from an apparent chaotic sequence of collisions[23]. Another useful technique implemented in optical microscopy is the localized laser-based Dynamic Light Scattering (DLS). DLS has been used to monitor changes in Brownian motion of Virus Like Particles (VLPs) in solution[24], giving information related to particle size and diffusion properties[23,25]. Viruses represent a simple or primitive self replicating organism, since viruses have genes and evolve by natural selection. Consequently they are exploited as the simplest biological model to study essential characteristic of living organisms[26] and the understanding of their self assembling represents a challenging task for biophysicists. Moreover, altered mechanical characteristics of tissues or single cell compartment may either correlate with or play an important role in the onset of pathology[27]. For example, changes in the compliance of blood vessels are associated with atherosclerosis, and changes of the mechanical properties of malignant cells[28] can be characterized by change of Brownian motion fluctuation in an optical trap[29].
The use of PFM and DLS to probe cells for quantitative biophysical parameters can represent an alternative descriptive marker for the onset and evolution of pathology.
Furthermore, optical tweezers open the field of single molecule manipulation and its biophysical characterization. With the appropriate chemistry a bead can be attached to a single molecule as a handle allowing the application of forces on the single molecule[30]. In conclusion, optical tweezers microscopy can be used for a wide range of experiments, from single molecule to cell level and help to understand their organization up to the tissue level.

Optical trapping principle and setups

The first demonstration that light radiation pressure induces forces on microparticles suspended in fluid was given by Arthur Ashkin in the early 70s[9]. He observed microparticles confined to the laser optical axis and pushed in the direction of propagation. Using two counter propagating laser beams the first three-dimensional trapping of a particle was demonstrated. Later, in 1986, Ashkin and his colleagues demonstrated the single beam gradient force optical trap using a single laser beam tightly focused by a high numerical aperture (NA) objective[31,32], which is at the base of most of the optical trapping setups of our days. Interestingly to note, the optical tweezers technique reported in this paper was thought as a proof of concept for atom trapping[33], extensively investigated in that period at Bell laboratories and demonstrated in the same year.
Light carries both linear and angular momentum and can thus exert forces and torques on matter. Optical tweezers exploit this fundamental property to trap objects in a potential well formed by light. Optical traps involve the balance of two types of optical forces: scattering

forces, which push objects along the direction of propagation of the light and gradient forces, which pull objects along the spatial gradient of light intensity[32].

When gradient optical forces exceed those from scattering, an object is attracted to the point of highest intensity formed by focused light and can be stably trapped at this position in all three dimensions. Actually, since more particles are usually interacting in the laser beam, a third force is present: the binding force, which represents the self-consistent interaction between the multiple particles and the incident wave[32].

The trapping force, F, is proportional to the power of the laser, W, and the refractive index of the fluid, n_m:

$$F = Q\frac{n_m W}{c} \qquad (1)$$

where c, is the velocity of light and Q, is a dimensionless coefficient expressing the efficiency of the trap and depending on a series of factors as the material and the shape of the particle[32].

In order to get a feeling of the level of the forces induced by the laser radiation pressure, let us consider the following simplified example: given a spherical particle (bead) of diameter d= 1μm, which totally reflects the incident laser beam of power W= 1mW, we want to estimate the force, F_p, exerted on the particle and the acceleration, a, of the particle[34]. Considering the linear momentum of a photon, p, the number, N, of photons/second carried in the laser beam and the variation of the momentum by total reflection, the force, F_p, is:

$$F_p = \frac{dP}{dt} = N2p = 2W/c = 10\,pN \quad (2)$$

where P is the momentum of the laser beam, and c the velocity of light.

This force is very small, but since also the particle is small (its mass, m ~10^{-12} grams), the acceleration, a= 1000 g (where g is the gravitational acceleration) is very big. Even if we consider losses in the reflection, and a force of only F_p= 1 pN, the acceleration of the particle a= 100 g is still big.

A detailed investigation of the trapping mechanism and forces can be approached considering the size ,d, of the trapped particle with respect to the wavelength, λ, of the trapping laser. There are three cases:

1. $d >> \lambda$ 2. $d << \lambda$ 3. $d \sim \lambda$

The ray optics approach can be applied for the first case, assuming the laser beam is described by rays which refract and reflect at the interface particle-fluid and considering the changes of the linear momentum associated to these laser rays[34].

If $d << \lambda$ (case 2), the particle in the laser focus can be thought as a dipole in the electromagnetic field and the radiation forces can be derived considering the Rayleigh scattering regime[35].

When the size of the particle is about the laser wavelength (case 3), the above mentioned approaches with their approximations can not be applied and a rigorous theory of the electromagnetic field governed by Maxwell's equations should be considered. The force of the electromagnetic field (e-m filed) when impinging on the particle can be computed either via a direct application of the Lorenz force and bound/free current/charges within the volume of changes or via the Maxwell stress tensor. The second approach has the advantage of computation efficiency since the e-m fields need to be evaluated only on a surface enclosing

the object, while the first method requires the evaluation of the fields within the whole volume. However, the disadvantage of the second method is that the polarizability of the object within its volume is not computed[36]. Different techniques to compute the forces in these regime are reported[37-42].

From the point of view of the optical setup, a single trap optical tweezers system is a relatively simple optical architecture to adapt to an optical microscope. The trapping laser beam is collimated and expanded to slightly overfill the pupil aperture of the microscope objective. The laser beam is coupled to the optical axis of the microscope through an appropriate dichroic mirror[43]. A high NA objective (NA>1) is required to obtain a high gradient of the intensity in the focal plane. Oil immersion objectives with NA as high as 1.4 and even higher for TIRF objectives can be used but the drawback consists in the presence of important spherical aberrations. Therefore water immersion objectives having NA up to 1.2 are preferred. To change the position of the trapped object, two mirrors can be used to deflect the laser beam. However this implies a reduced efficiency of the trap when the trapping position is moved from the objective focus. An alternative is to move the sample cell and keep the particle fixed in the focal point. This allows to change the relative position of the particle to the surrounding environment with no change in the optical path of the beam and, hence, keeping the optical properties of the trap unaffected. Scanning the beam in the sample is more cumbersome: the mirrors and the pupil aperture of the objective need to be optically conjugated by a telescope. Such system has the drawback that the trap position can be only controlled in the x, y directions. To move the trap in the z direction the stage should be moved. Another approach is to change the distance between the lenses of the beam expander: the collimation of the beam at the entrance of the microscope objective is varied and, consequently a change in the equilibrium between the scattering and the gradient force produces a shift of the relative position of the trapped object respect to the objective focus[44].

To increase the number of trapping spots in the sample more than one laser can be used. Alternatively, a single beam can be split by a polarizing beam splitter cube and slightly shift the second beam respect to the first[45]. Such kind of solution allows a maximum of two traps for each laser beam. Many laboratories in the last decade have been improving their optical setups to obtain multitrapping in the sample and increase the manipulation capabilities. Two kinds of approaches have been practically used. One is based on acousto-optical devices[46], which are able to fast steer the laser beam on different positions which time share the light power, so that trapped objects don't feel the scanning of the laser. Another lies on diffractive optical elements that reshape the Gaussian beam of the laser in an arbitrarily shaped intensity profile to obtain the desired trapping configuration on the sample[47]. The first approach permits to change the number and position of spots at high speed, but trapping spots are created only in planar arrangement. The second method requires higher computational skills, but allows to obtain a three dimensional array of trapping spots, or more complex shapes of trapping spots[48]: e.g., Bessel beams are "non-diffracting" and they propagate without much spreading trough obstacle[49], Laguerre-Gauss beams can transfer their angular orbital momentum on trapped particles or they can trap low refractive index probes as bubbles[50,] anisotropic beam shapes create a potential which influence molecular dipole diffusion and distribution and they could influence cell growth[51]. Recently this technique based on diffractive optical elements has been

transferred to microfabricated solid supports, i.e., presenting high NA Fresnel lenses built on the coverslip, to trap particle without even the need of a microscope objective[52].

Once the optical tweezers are built, they can be calibrated, as discussed in the next section, to obtain the stiffness of the optical trap and perform force measurements. To calibrate the optical tweezers system it is necessary to measure with high accuracy the displacement of the trapped probe from the equilibrium position in the trap. One method is to use video tracking. Optically resolved probes can be tracked by simple brightfield imaging applying centroid algorithms, while subresolved probes can be tracked if they emit fluorescent light[53]. In such kind of setup no additional hardware is required and particle position measurements can be obtained with accuracy of the order of 10 nm and a bandwidth of few kilohertz. Video tracking is a simple method to calibrate the stiffness of a single- or multi-trap configuration. Furthermore when the detection path of the system is modified to project a video hologram (and not an image) to the CCD, tracking of the probe reach nanometer resolution and its refractive index can be measured with high accuracy[54].

Another popular method to track the probe position is based on light interferometry measurements[55]. This configuration measures the interference between the light scattered by the trapped object and the unscattered light passing through the focus. The interference pattern is collected at the back focal plane of the condenser and projected to a position sensitive detector[56]. This detector can be either a position sensitive detector (PSD) which is able to track arbitrary shape objects in the x, y direction, or a quadrant photodiode (QPD) which is able to track a symmetric probe in three directions (x,y,z). In this kind of measurements, both types of detectors permit to combine sub-nanometer resolution with a temporal bandwidth of hundreds KHz. Another important issue in the setup is the noise. PFM is sensible to any kind of environmental noise: thermal, acoustic, convective. Therefore the sensitivity of the system can be improved by closing off the setup into an acoustic chamber, which also reduce convective noise, and by controlling the environmental temperature. Furthermore, feedback control on the output intensity of the laser or feedback control in the stage position to reduce mechanical drift of the sample permit to reach sub nanometer displacement resolution and femtonewton force resolution[57,58].

Optical trap calibration

Optical manipulation setup started to be used as force transducers in after 1989, when Block[12], made the first calibrated measurement of the compliance of bacterial flagella, using the tweezers to force bacteria to rotate (they were tethered to a microscope cover-glass by their flagellum).

To calibrate the optical force of the system it is necessary to take into account all external forces acting on the trapped probe. Starting from Ornstein and Uhlenbeck[59] equation to describe the trajectory of an object:

$$m\ddot{x}(t) = -\gamma\dot{x}(t) + F_{Brownian} \quad (3)$$

where m is the inertial mass of the particle, while the Stokes friction $-\gamma\dot{x}(t)$ and the random Brownian force represent the surrounding medium influence on the object trajectory. The Brownian forces acting on the trapped probe can be modeled as: $\sqrt{2D\gamma}h(t)$, where D is the

diffusion coefficient, γ is the friction coefficient, and h(t) is an independent white Gaussian random processes.

In an optical trap, the electric field of the laser radiation produce forces on charged particles, consequently the motion of the induced dipole, arising from the electronic polarizability of the trapped particle, it is also affected by the potential well of the laser radiation. From the distribution histogram of the particle position in the trapping volume it can be shown that the potential is harmonic: when the potential is harmonic, such distribution should be Gaussian[7]. This permits to model the optical forces as a spring: $F_{opt} = -kx$, where *k* is the optical stiffness and *x* it is the probe displacement from the equilibrium position[34]. Thus equation (4) becomes:

$$m\ddot{x}(t) = -\gamma\dot{x}(t) + F_{Brownian} + F_{Opt} \quad (4)$$

In this equation, the inertial term can be neglected since low Reynolds number conditions apply.

Once the equation of motion of a trapped object is modeled, the optical stiffness of the system can be obtained by measuring the probe displacements in the trap. Different methods have been implemented to calibrate the optical tweezers and they are based on some *a priori* information. The tolerance on such parameters produce the accuracy of the calibration method applied.

The drag force method can be applied by video or laser interferometric tracking. The drag coefficient, including surface proximity corrections, should be known *a priori*. In this method a force is generated on the trapped probe by a fluid flow, and the trapped bead response is measured as the distance between the new equilibrium position and the trap center. Although the lateral displacement of the object due to the drag force is relatively easy to measure by video tracking, axial displacements represent a more difficult task. To measure the probe position in the z direction by video tracking, the bead image can be calibrated[60] by its fluorescence intensity, if acquired in a confocal setup, or by the diameter of the airy disk pattern in a widefield microscope[53].

Other methods rely on the Brownian motion detection of the trapped probe and simple video tracking doesn't have the required spatial and temporal resolution. Therefore interferometric measurements are applied[56].

In the equipartition method the kinetic energy of the trapped object is assumed equal to the thermal energy:

$$\frac{1}{2}k_B T = \frac{1}{2}k\langle x^2\rangle \quad (5)$$

Where k_BT is the thermal energy, and *k* the optical stiffness.

In such equation the temperature T is the *a priori* parameter. In addition, a separate calibration of the detector transduction from volts to nanometers has to be performed separately.

In the power spectrum method such calibration of the detector is not required and Boltzmann statistics is directly applied to the power spectrum of the position fluctuations of the probe, measured in volts by the PSD or QPD. In such method the fit with a Lorentzian function is applied to the power spectrum (measured in $Volt^2/Hz$) to obtain the optical stiffness and sensitivity of the detector (in Volt/nm). The temperature and the viscosity of the surrounding medium have to be known *a priori*.

The power spectrum method is the most applied because it permits a fast calibration of the system: PSDs and QPDs permit to measure position fluctuation with a temporal bandwidth of

hundreds of KHz and therefore few seconds of recordings are enough to obtain sufficient data points. This means that optical tweezers can be calibrated easily at the environmental condition in the sample.
In fact it is well known that optical properties of the sample affect optical characteristic of the setup, as its Point Spread Function (PSF), and therefore its trapping efficiency.
The drawback of the method is that it relies on two parameters that have to be known *a priori* and therefore they decrease the accuracy.
Interferometric recordings give the possibility to resolve Brownian motion and to observe hydrodynamic effect on medium viscosity[59]. Therefore they were taken into account in data analysis to obtain a better estimate of the optical stiffness of the system. Also mathematical modeling of optical system may improve the performances: low pass filtering effect of the detector[61], shape of the trapping potential at the focus spot, condenser NA influence on the instrument sensitivity were modeled[62,63] and the local shift variance sensitivity of the QPD were measured[64]. Such studies represented an important contribution to obtain system calibration and achieve high sensitivity[65].
Therefore, the accuracy limit in the calibration of the system is due to the *a priori* parameters that need to be included in the data analysis. This has been overcome by a new calibration strategy where two methods are combined to obtain experimental parameters of the probe without the need of *a priori* information. The method relies on power spectral measurements of thermal motion of the probe during a sinusoidal motion of a translation stage. This method allows the extrapolation of the parameters, that are used as *a priori* information in the procedures described above, with accuracy within 3% [57], and it has been applied to resolve surface forces which can be an important issue at biological interfaces as membranes. Furthermore the method has been used to calibrate the detector sensitivity for particles tracking inside the cell[66,67], which can represent a first step to the challenging field of intracellular force measurements.

Optical Tweezers versus Fluorescence Microscopy

Lukosz's principle[68] states that resolution can be increased at expense of the field of view.
Fluorescence microscopy gives the possibility to observe only the compartment marked in the sample and therefore provides a better contrast respect to the overall specimen. Further technological improvements in optical microscopy reduce even more the field of view, e. g., in the confocal architecture, which confers higher spatial resolution in the two-dimensional field of view and allows access to the third dimension of the sample. Many confocal architectures have been implemented[69]: in the one photon confocal microscope, the field of view is decreased in the detection path, while in two-photon microscope such confinement is obtained in the excitation process. Both types of confocal microscopes give the possibility to observe a small volume (the detection volume is in the order of femtoliters) and supply the possibility to observe single fluorescent molecules[70]. Many efforts have been spent to reduce the spatial dimensions of the Point Spread Function of the confocal systems to overcome the diffraction limit and develop the nano-scope[3,71] for the application of molecular imaging to living systems.
The relatively limited spatial resolution of optical microscopy is counter balanced by the multi dimensionality of the data acquired: e.g., time lapse imaging of a 3D volume allows exploiting a

fourth dimension. Moreover, the wavelength, λ, enables multi labeling and discrimination of different entities in the sample. Spectral properties of fluorochromes such as the lifetime of the excited state, give information on the environmental condition of the molecule[72]. Changes in the intracellular environment, related to the cell metabolism, can influence the structure of the fluorescent molecules and their optical properties[73]. Therefore, cells physiology can be studied at molecular level. This is the so called lifetime dimension. Furthermore, the Second Harmonic Generation, occurring when an intense laser beam passes through a polarizable material with non-centrosymmetric molecular organization, gives another possible dimension for optical microscopy measurements[74].

The photonic force microscope, add one more controlled or measurable[75] variable to optical microscopy: the force. Therefore optical tweezers represent a further resolution improvement for the optical microscope: force measurements permit to follow polymerization steps of single filaments, where the added monomer raises the length of the polymer of some nanometers[76], or Brownian motion analysis can be applied to resolve 3D structures with 10 nm resolution[77].

Laser tweezers is highly compatible with optical microscopy techniques because it exploit the same optical path[43], however, it induce photodamage, which arise from the exposure of the trapped sample to high intensity of light[78]. To overcome this problem it is possible to decrease the intensity reaching the sample, if a better trapping efficiency of the system is reached. For example by adaptive optics methods it is possible to recover non ideal behavior of the objective lens to obtain unblurred focus spots and better spatial confinement of photons[79].

Such method to improve the trapping efficiency is similar to deconvolution processing of microscopy images to improve the experimental spatial resolution of microscopes[80,81]. In such technique it is necessary to characterize the optical system by its Optical Point Spread Function[2] (OPSF). In this respect, theoretical modeling can characterize the image formation process of the microscope, but only experimental measurements of the PSF can quantify the limitations of the real system[82]. Indeed, experimental OPSF presents shape asymmetry due to spherical aberrations introduced by optical elements, while theoretical OPSF is symmetric and account only for the resolution limits of an ideal imaging system[83]. The disadvantage of experimental OPSF is that could be corrupted by noise, otherwise deconvolution with the theoretical OPSF offer only a qualitative enhancement of the image, because the introduced artifacts cannot be quantified.

In photonic force microscopy the Brownian motion of the trapped probe follow the shape of the potential well created by the focused laser which represents the Force Point Spread Function (FPSF) of the optical tweezers (Figure 1). If the trapped probe is tracked for enough time it is possible to measure the trapping volume with nanometer resolution and therefore define the spherical aberration of the system with the same accuracy[84,85]. It has been already proved that spherical aberrations produce enlargement of the OPSF[86,87]; and that recovering of such spherical aberrations by adaptive optics produce a smaller trapping volume, which represent less Brownian noise in force spectroscopy measurements and better trapping efficiency[79]. Techniques as photo-activated localization microscopy (PALM) and stochastic optical reconstruction microscopy (STORM) apply a fit between the PSF of the system and the point like features of the image to obtain the centre of mass of the labeled molecule at 20nm resolution[71].

In this context trapping efficiency is used as a quantitative parameter to estimate the optical spherical aberrations recovering by hardware deconvolution, the adaptive optics method[88]. This recovering could be also quantified by experimental fluorescent point spread function acquisition, which then it can be used in a software deconvolution algorithm[89].
Therefore correlation of force and fluorescence intensity data could improve the calculation of an experimental OPSF; while combination of hardware and software deconvolution can be applied to recover both type of errors in an optical system: degradation due to the process of image formation usually denoted as blurring, and degradation introduced by recording process usually denoted as noise[89].
In turn this can be exploited to obtain a higher single molecule localization accuracy of a STORM microscope[90].
Another way to decrease phototoxicity is the use of a laser source in the wavelengths window for which the absorption of the biological matter is low. The typical wavelength used for biological applications is in the infrared range for which it has been shown by means of viability tests both on bacteria and eukaryotic cells, that the damage versus exposure time is reduced[78,91]. Since the best wavelength range for trapping is the same used in two photon excitation, some groups started to use femto-second pulsed laser source to obtain trapping, ablation and fluorescence excitation by using only one beam[92,93].
In conclusion, by optical tweezers technique, it is possible to trap particles starting from single molecule, to living cells and confine them in a sub-diffraction limited volume which can be observed with an extended area detector[94]. Therefore, in principle, it is possible by optical tweezers to reduce the field of view of the system with no need of a pinhole in front of the detector, or an infrared femto-second pulsed laser to confine the excitation in a 3D volume. For example, such possibility can be exploited in fluorescence techniques as fluorescence correlation spectroscopy[95], or for single-molecule studies: Bustamante was the first scientist who used such technique to manipulate single molecule of DNA[96]. After his seminal paper many works followed on single molecule biophysical characterization[21] and application of single molecule manipulation in combination with fluorescence techniques[97,98].

Optical Tweezers in Biology

Cells need to organize their internal space and interact with their environment.
The network filaments, i.e., the cytoskeleton, represent connections to distribute tensile forces through the cytoplasm to nucleus as a signaling pathway[99]. Transmembrane receptor, as integrins, function as mechanoreceptors and provide a preferred path to transfer mechanical forces across cell surface[100]. During motion, cells organize integrins distribution in clusters at special complexes called focal adhesions[20]. Forces transmitted to the cytoskeleton from these sites produce a stress in associated cytoskeleton molecules which can be converted in gene expression, protein recruitment at local sites and dynamic cytoskeleton architecture modulation[101,102]. Thus cell shape and stability is the effect of a mechanical force balance between cytoskeleton traction forces and extracellular substrate local rigidity[19,99].
Regulation of assembly processes modulate dynamically the mechanical properties of the cytoskeleton network, locally and globally to balance compression and tension force, to extend

cell protrusions such as lamellipodia and filopodia, or to propel intracellular vesicles or pathogens through the cytoplasm[103].

For cells moving through tissues, the resistive force is coming from the surrounding extracellular matrix. For cells in vitro, the major force against extension arises from tension in the plasma membrane which modulates the shape of extruding processes[104,105].

In force spectroscopy measurements, the membrane elasticity has been quantified by tether extraction of membrane-embedded beads[106] and piconewton tensions have been applied to the phospholipids bi-layer to stimulate receptor membrane trafficking[107,108].

An important factor in membrane resistance is the number of membrane–cytoskeleton adhesion components. It has been shown that the force needed to extract a membrane tether can be modified by alterations of the cytoskeleton[107,109]. It was also demonstrated that mechanical stimuli, which induce membrane tension changes, can regulate membrane traffic through exocytosis and endocytosis[108]. These results are in agreement with observations of normal behavior of the cell, for example: during endocytosis, clathrins displace the membrane-associated cytoskeleton to decrease membrane tension and to cause membrane engulfment[105]. In the case of membrane protrusion, the displacement of the normal cytoskeletal components is required to create a gap for the insertion of new monomers at the filament tips[110].

Apparent membrane tension, which is in the order of tens of pN, have been measured from the force exerted on membrane tethers[106]. An analysis of the tether-formation processes is important because it allows calculating the bending rigidity of membranes, the apparent surface tension, and therefore to obtain a theoretical model of the force produced or the energy dissipated during motion. Furthermore optical tweezers can also be used to track membrane proteins with no need of fluorescent marker at unraveled resolution[111]. For example receptor tracking permitted to distinguish differences in membrane fluidity in living and dead cells[112].

The membrane deform passively in response to cytoskeleton reorganization.

Since actin filaments are rather fragile, mechanical properties of a single actin fiber is difficult to measure. Microtubules are much stiffer, and force generation by this polymer has been measured by observing how a single microtubule buckles when polymerizing against a wall. This permitted to follow polymerization steps of single filaments and demonstrated that a microtubule growing at the ‘plus end’ develops a force of a few piconewtons and that polymerization velocity decreases exponentially as a function of the load force[45]. In addition, microtubules are long filamentous proteins structures that alternate between periods of elongation and shortening in a process termed dynamic instability[76]. The average time a microtubule spends in an elongation phase, known as the catastrophe time, is regulated from the biochemical machinery of the cell and a comparison of catastrophe times for microtubules growing freely or in front of an obstacle leads to conclusion that force reduces the catastrophe time by limiting the rate of tubulin addition.

Although actin filament is less stiff then microtubules, it represents an essential component in cellular motility: it provides protrusive forces to extend cell protrusions such as lamellipodia and filopodia, or to propel intracellular vesicle or pathogens through the cytoplasm[113]. The forces generated by elongation of a few parallel-growing actin filaments against a rigid barrier, mimicking the geometry of filopodial protrusion, has been measured[114,115], and it was shown that growth of approximately eight actin parallel-growing filaments can be stalled by relatively

small applied load forces on the order of 1 piconewton. These results suggest that force generation by small actin bundles is limited and therefore living cells must use actin-associated factors to generate substantial force to overcome membrane resistance[116] and to produce stable protrusions at the leading edge of the cell during locomotion[117].

Another important role that the cytoskeleton plays in cell physiology is the intracellular transport of various cargos. In intracellular transport two aspects have to be analyzed: one is how cargos use the network and the second is how the cell changes the structure of the networks to assist cargo motion. Pathogens have been used as simplified model systems to study eukaryotic cell motility. In vitro monitoring of their movement in cell extracts converted a complex cell biology problem into a biochemically affordable problem, and opened the way to design a minimal motility medium to study the biochemical mechanism of actin dynamics control[118].

One of the most important recent discoveries about the actin propulsion is the proof that the actin tail is attached to the surface of the pathogens[119]. Noireaux[120] used an optical trap to measure the force required to separate the bacterial cell from the actin tail, which turned out to be greater than 10 piconewton. Finally, Cameron[121] used electron microscopy to observe that actin filaments of the branching network are transiently attached to the surface of the bead. This leads to more widely accepted model: the elastic tethered ratchet model[122], in which attached fibers are in tension and resist the forward motion of the bacterium/bead, while dissociated fibers are in compression, and generate the force of propulsion.

Recently atomic force microscopy (AFM) measurements have succeeded in stalling actin network growth and revealed that two or more stable growth velocities can exist at a single load value. These results demonstrate that a single Force-Velocity relationship does not describe completely the behavior of the system which depends on loading history and not only on the instantaneous load[123]. Another experiment reports the effort to stop motion of Listeria with an optical trap[114,124]. It has been shown that the trap could temporarily stop its motion, and then the bacterium escapes due to an increase in the force supplied by the tail, like in an autocatalytic model[125]. Autocatalytic model is also sustained by measurements with fluorescent actin, where it has been shown that the fluorescence intensity in actin tail, increases during the stationary period of the bacteria motion, suggesting that the actin density is building up to overcome the opposing forces[126].

Optical tweezers can be also utilized to measure and analyze the force operated by cells[127] in exploratory motion and therefore to understand how cell operate mechanic transduction. With optical microscopy, it is possible to follow the motion of the cell, but force measurements permit to quantify how many molecular motors are involved in a movement and therefore to quantify how much the molecular machinery of the cell is recruited in such action. This means that thanks to force measurement, it is possible to distinguish random motion from well organized shift of the cell (Figure 2)[128].

It has been observed that filopodia, which explore the environment by rapidly moving in all directions, modulate their activity changing the duration of the collision with a bead, in response to different stiffness of the load. This could represent sensing of the obstacle force and is in agreement with measurements on single microtubule catastrophic time modulation[76].

Lamellipodia, which follow the pathway analyzed by filopodia, showed a more complex behavior in response to the obstacle: sometimes, they entirely retracted, other times they

moved around it to progress forward or they removed the obstacle by lifting it and giving it back (Figure 3). Lamellipodia have a more differentiated structure and are thought to exert a force with variable directions in space. Therefore, multi-tweezers measurements have been applied[129] to understand their overall organization and to measure complex forces exerted during growth cone motion.

This kind of measurements can be used to understand the response of the cells to molecular cues or mechanic-chemical stimuli[130] localized in the trapping volume, or to understand the mechanisms and which molecules are involved in different steps of motor planning.

Single biological particles, usually used as simple biological models, have been also trapped: Tobacco mosaic virus, Escherichia coli bacteria, and manipulation of particles within the cytoplasm of cells[131]. Optical tweezers became also a well-established technique for single-molecule studies: Bustamante was able to follow the DNA encapsidation steps of the bacteriophage and to measure the force delivered by capsid molecular motors[132]. Study of single molecular motors is one of the most attractive applications of optical tweezers: the forces generated by single motor molecules such as kinesin and myosin has been quantified[133,134] or steps of RNA Polymerase along DNA filaments have been measured[135].

A complementary system to light manipulation tools that is fast evolving is laser dissection[136]. By laser scissors it was possible to cut living biological samples with subcellular resolution: the cytoskeleton organization could be disturbed while leaving the cells unaffected in any other respect[137]. Optical tweezers and laser dissection tools were also used to control the location and timing of optical uncaging in chemical stimulation experiments[138], or for optoporating the cell membrane[139,140]. These opportunities encourage the use of optical tools in probing and quantifying biophysical cellular parameters, and open the new field of nanosurgery[92,141].

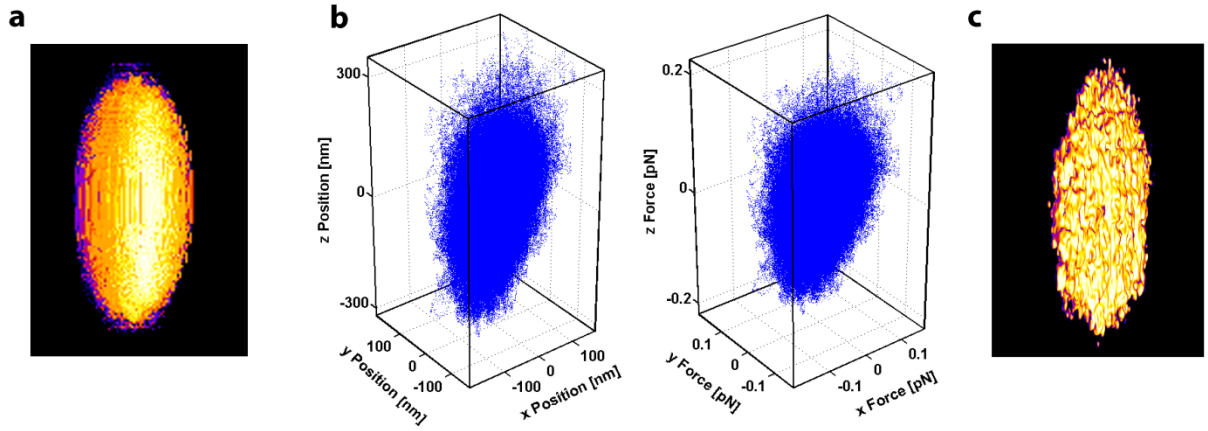

Figure 1. Optical and Force Point Spread Function.

Three dimensional rendering of an Optical point spread function of a confocal microscope (objective 100X NA 1.4 oil immersion) measured with 64nm diameter latex beads immersed in oil. Field of view 0.8 x 1µm. **(a)**. Three dimensional scatter plots of 1µm diameter silica bead, trapped with a CW infrared laser (1064 nm wavelength, objective 100X NA 1.4 oil immersion) in

water. Scatter plots are computed from the x, y, z trace, in nm and pN, low pass filtered at 20KHz and acquired at 10KHz**(b).** Three dimensional rendering of a Force point spread function representing the volume observed from the trapped object. Field of view 0.8 x 1µm **(c)**.

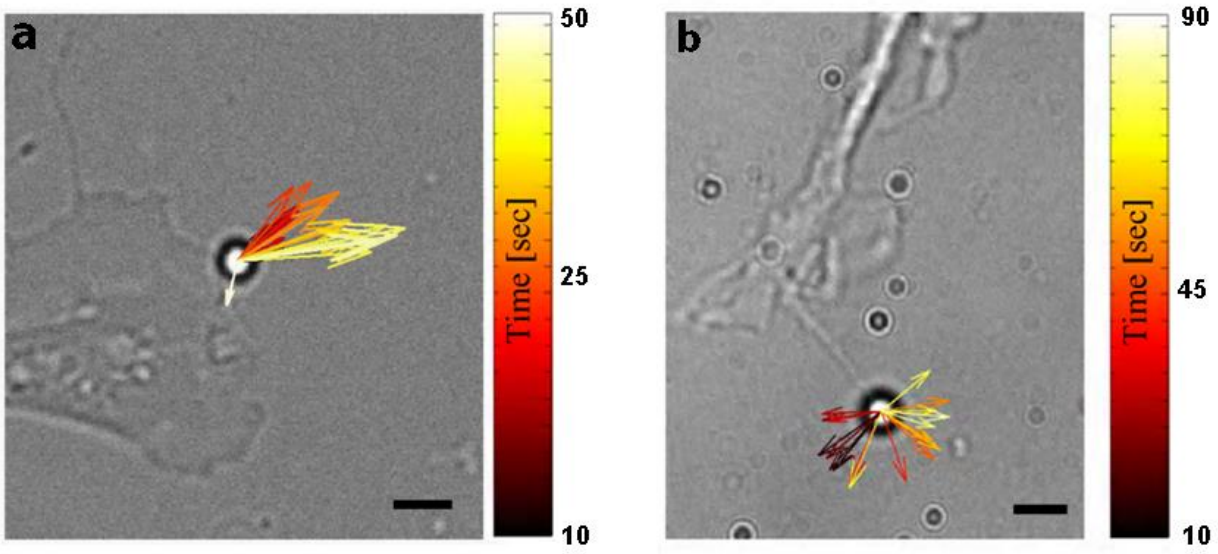

Figure 2. Force measurement and cell motility.
Vectorial representation of the force exerted by the cell on obstacle (1 µm diameter silica bead). Different colors of the vector represent different time at which cell exerts the force on the trapped probe. In **(a)** lamellipodium increase the force exerted on the obstacle and tries to avoid it, as suggested from the time evolution of the length and direction of the force. In **(b)** the random succession of force vector direction in time represents the exploratory motion of a filopodium which senses the environment. Bars 2 µm.

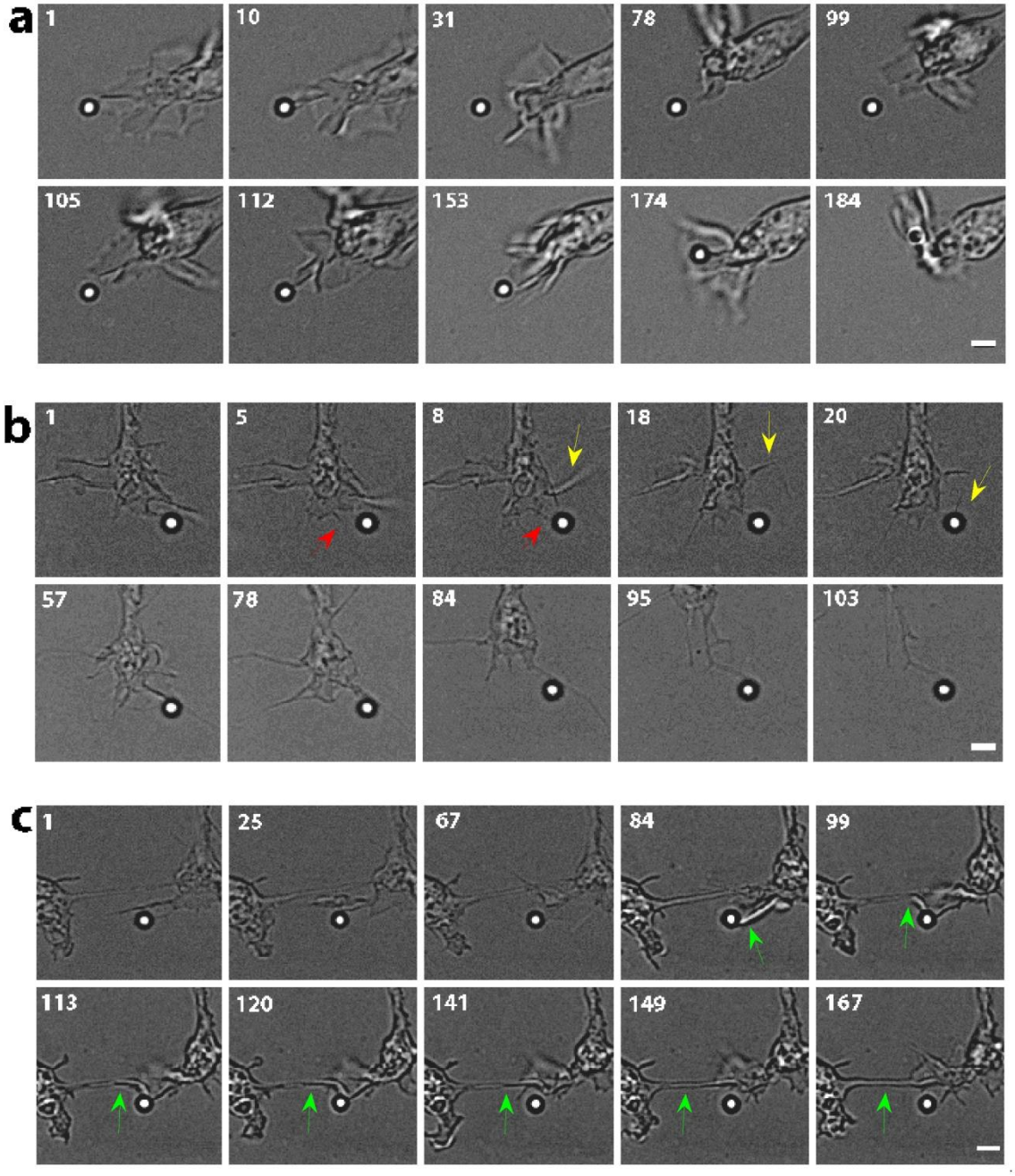

Figure 3. Cell behavior in front an obstacle.
In **(a),** the growth cone senses the load, retracts and grow again toward the obstacle to remove it. In **(b),** the growth cone senses the load, and completely retracts. Red and yellow arrows indicate the growing filopodia which retract and bend toward the obstacle. In **(c)** a bead is trapped between two connected growth cones. Lamellipodium of the growth cone on the right side is attracted from the load, but then avoid the obstacle. Green arrows indicate how the connection between the two growth cone is reinforced when the lamellipodium of the growth cone on the right side stops to push the trapped probe and steer toward the connection between the two neurites. Bars 2 μm.

Reference List

1. Diaspro,A. *et al.* Multi-photon excitation microscopy. *Biomed. Eng Online.* **5**, 36 (2006).
2. Diaspro,A., Annunziata,S., Raimondo,M. & Robello,M. Three-dimensional optical behaviour of a confocal microscope with single illumination and detection pinhole through imaging of subresolution beads. *Microscopy Research and Technique* **45**, 130-131 (1999).
3. Hell,S.W. Far-field optical nanoscopy. *Science* **316**, 1153-1158 (2007).
4. Hell,S.W. Microscopy and its focal switch. *Nat. Methods* **6**, 24-32 (2009).
5. Huang,H., Kamm,R.D. & Lee,R.T. Cell mechanics and mechanotransduction: pathways, probes, and physiology. *Am. J. Physiol Cell Physiol* **287**, C1-11 (2004).
6. Lahenkari,P.P. & Horton,M.A. Single integrin molecule adhesion forces in intact cells measured by atomic force microscopy. *Biochem Biophys Res Commun* **259**, (1999).
7. Erikson,H.P. Reversible unfolding of fibronectin type III and immunoglobulin domains provides the structural basis for stretch and elasticity of titin and fibronectin. *Proc Natl Acad Sci USA* **91**, (1994).
8. Finer,J.T., Simmons,R.M. & Spudich,J.A. Single myosin molecule mechanics: piconewton forces and nanometre steps. *Nature* **368**, 113-119 (1994).
9. Ashkin,A. Acceleration and Trapping of Particles by Radiation Pressure. *Physical Review Letters* **24**, 156-& (1970).
10. Moffitt,J.R., Chemla,Y.R., Smith,S.B. & Bustamante,C. Recent advances in optical tweezers. *Annu. Rev. Biochem.* **77**, 205-228 (2008).
11. Macdonald,M.P. *et al.* Creation and manipulation of three-dimensional optically trapped structures. *Science* **296**, 1101-1103 (2002).
12. Block,S.M., Blair,D.F. & Berg,H.C. Compliance of Bacterial Flagella Measured with Optical Tweezers. *Nature* **338**, 514-518 (1989).
13. Neuman,K.C. & Block,S.M. Optical trapping. *Review of Scientific Instruments* **75**, 2787-2809 (2004).
14. Peyton,S.R., Ghajar,C.M., Khatiwala,C.B. & Putnam,A.J. The emergence of ECM mechanics and cytoskeletal tension as important regulators of cell function. *Cell Biochemistry and Biophysics* **47**, 300-320 (2007).
15. Pampaloni,F., Reynaud,E.G. & Stelzer,E.H. The third dimension bridges the gap between cell culture and live tissue. *Nat. Rev. Mol. Cell Biol.* **8**, 839-845 (2007).
16. Bakunts,K., Gillum,N., Karabekian,Z. & Sarvazyan,N. Formation of cardiac fibers in Matrigel matrix. *Biotechniques* **44**, 341-348 (2008).
17. Riveline,D. *et al.* Focal contacts as mechanosensors: Externally applied local mechanical force induces growth of focal contacts by an mDia1-dependent and ROCK-independent mechanism. *Journal of Cell Biology* **153**, 1175-1185 (2001).
18. D.E.Ingber. **Tensegrity I. Cell structure and hierarchical systems biology**. Journal of Cell Science 116, 1157-1153. 2003.

Ref Type: Generic

19. Giannone,G. *et al.* Lamellipodial actin mechanically links myosin activity with adhesion-site formation. *Cell* **128**, 561-575 (2007).
20. Galbraith,C.G., Yamada,K.M. & Galbraith,J.A. Polymerizing actin fibers position integrins primed to probe for adhesion sites. *Science* **315**, 992-995 (2007).

21. Bustamante,C., Bryant,Z. & Smith,S.B. Ten years of tension: single-molecule DNA mechanics. *Nature* **421**, 423-427 (2003).
22. Coirault,C., Pourny,J.C., Lambert,F. & Lecarpentier,Y. [Optical tweezers in biology and medicine]. *Med. Sci. (Paris)* **19**, 364-367 (2003).
23. Santos,N.C. & Castanho,M.A. Teaching light scattering spectroscopy: the dimension and shape of tobacco mosaic virus. *Biophys. J.* **71**, 1641-1650 (1996).
24. Pattenden,L.K., Middelberg,A.P.J., Niebert,M. & Lipin,D.I. Towards the preparative and large-scale precision manufacture of virus-like particles. *Trends in Biotechnology* **23**, 523-529 (2005).
25. Meller,A. *et al.* Localized dynamic light scattering: a new approach to dynamic measurements in optical microscopy. *Biophys. J.* **74**, 1541-1548 (1998).
26. S.J.Flint, L.W Enquist, R.M.Krug, V.R.Racaniello & A.M.Skalka. Principle of Virology. Molecular Biology, Pathogenesis, and Control. (2000).
27. Berrier,A.L. & Yamada,K.M. Cell-matrix adhesion. *Journal of Cellular Physiology* **213**, 565-573 (2007).
28. Guck,J. *et al.* Optical deformability as an inherent cell marker for testing malignant transformation and metastatic competence. *Biophys. J.* **88**, 3689-3698 (2005).
29. Anna Chiara De Luca *et al.* Real-time actin-cytoskeleton depolymerization detection in a single cell using optical tweezers. *Optics Express* **15**, (2007).
30. Bustamante,C., Smith,S.B., Liphardt,J. & Smith,D. Single-molecule studies of DNA mechanics. *Current Opinion in Structural Biology* **10**, 279-285 (2000).
31. Ashkin,A., Dziedzic,J.M., Bjorkholm,J.E. & Chu,S. Observation of A Single-Beam Gradient Force Optical Trap for Dielectric Particles. *Optics Letters* **11**, 288-290 (1986).
32. Burns,M.M., Fournier,J.M. & Golovchenko,J.A. Optical binding. *Phys. Rev. Lett.* **63**, 1233-1236 (1989).
33. Ashkin,A. Optical trapping and manipulation of neutral particles using lasers: a reprint volume with commentaries. (2006).
34. Ashkin,A. Forces of a single-beam gradient laser trap on a dielectric sphere in the ray optics regime. *Methods in Cell Biology, Vol 55* **55**, 1-27 (1998).
35. Harada,Y. & Asakura,T. Radiation forces on a dielectric sphere in the Rayleigh scattering regime. *Optics Communications* **124**, 529-541 (1996).
36. MIT Center for Electromagnetic Theory and Applications. http://web.mit.edu/~ceta/obt/fund-forces.html . web site . 2009.
37. M.Mansuripur. Radiation pressure and the linear momentum of the electromagnetic field. *Opt. Express* **12**, (2004).
38. B.A.Kemp, T.M.Grzegorczyk & J.A.Kong. *At initio study of the radiation pressure on dielectric and magnetic media*. *Optics Express* **13**, (2005).
39. J.P.Gordon. Radiation forces and momenta in dielectric media. *Phys. Rev. A* **8**, (1973).
40. R.Loudon. Theory of the radiation pressure on dielectric surfaces. *J. Mod. Opt.* **49**, (2002).
41. Y.N.Obukhov & F.W.Hehl. Electromagnetic energy-momentum and forces in matter. *Phys. Lett. A* **311**, (2009).
42. Rohrbach,A. & Stelzer,E.H. Trapping forces, force constants, and potential depths for dielectric spheres in the presence of spherical aberrations. *Appl. Opt.* **41**, 2494-2507 (2002).
43. Lee,W.M., Reece,P.J., Marchington,R.F., Metzger,N.K. & Dholakia,K. Construction and calibration of an optical trap on a fluorescence optical microscope. *Nat. Protoc.* **2**, 3226-3238 (2007).
44. Kress,H., Stelzer,E.H., Griffiths,G. & Rohrbach,A. Control of relative radiation pressure in optical traps: application to phagocytic membrane binding studies. *Phys. Rev. E. Stat. Nonlin. Soft. Matter Phys.* **71**, 061927 (2005).

45. Kikumoto,M., Kurachi,M., Tosa,V. & Tashiro,H. Flexural rigidity of individual Microtubules measured by a buckling force with optical traps. *Biophysical Journal* **90**, 1687-1696 (2006).
46. Visscher,K., Brakenhoff,G.J. & Krol,J.J. Micromanipulation by "multiple" optical traps created by a single fast scanning trap integrated with the bilateral confocal scanning laser microscope. *Cytometry* **14**, 105-114 (1993).
47. Dufresne,E.R. & Grier,D.G. Optical tweezer arrays and optical substrates created with diffractive optics. Review of Scientific Instruments. *Review of Scientific Instruments* **69**, (1998).
48. D.Cojoc *et al.* Dynamic multiple optical trapping by means of diffractive optical elements. *Microelectronic Engineering* **73-74**, (2009).
49. McGloin,D., Garces-Chavez,V. & Dholakia,K. Interfering Bessel beams for optical micromanipulation. *Opt. Lett.* **28**, 657-659 (2003).
50. Garbin,V. *et al.* Optical micro-manipulation using Laguerre-Gaussian beams. *Japanese Journal of Applied Physics* **44**, (2005).
51. Carnegie,D.J., Stevenson,D.J., Mazilu,M., Gunn-Moore,F. & Dholakia,K. Guided neuronal growth using optical line traps. *Opt. Express* **16**, 10507-10517 (2008).
52. Schonbrun,E. & Crozier,K.B. Spring constant modulation in a zone plate tweezer using linear polarization. *Opt. Lett.* **33**, 2017-2019 (2008).
53. Speidel,M., Jonas,A. & Florin,E.L. Three-dimensional tracking of fluorescent nanoparticles with subnanometer precision by use of off-focus imaging. *Opt. Lett.* **28**, 69-71 (2003).
54. Sang-Hyuk Lee *et al.* Characterizing and tracking single colloidal particles with video holographic microscopy. *Optics Express* **15**, (2007).
55. S Keen, J Leach, G Gibson & M J Padgett. Comparison of a high-speed camera and a quadrant detector for measuring displacements in optical tweezers. *J. Opt. A: Pure Appl. Opt.* **9**, (2007).
56. Gittes,F. & Schmidt,C.F. Interference model for back-focal-plane displacement detection in optical tweezers. *Opt. Lett.* **23**, 7-9 (1998).
57. Schaffer,E., Norrelykke,S.F. & Howard,J. Surface forces and drag coefficients of microspheres near a plane surface measured with optical tweezers. *Langmuir* **23**, 3654-3665 (2007).
58. Carter,A.R. *et al.* Stabilization of an optical microscope to 0.1 nm in three dimensions. *Appl. Opt.* **46**, 421-427 (2007).
59. Lukic,B. *et al.* Motion of a colloidal particle in an optical trap. *Phys. Rev. E. Stat. Nonlin. Soft. Matter Phys.* **76**, 011112 (2007).
60. Dreyer,J.K., Berg-Sorensen,K. & Oddershede,L. Improved axial position detection in optical tweezers measurements. *Appl. Opt.* **43**, 1991-1995 (2004).
61. Berg-Sorensen,K., Peterman,E.J.G., Weber,T., Schmidt,C.F. & Flyvbjerg,H. Power spectrum analysis for optical tweezers. II: Laser wavelength dependence of parasitic filtering, and how to achieve high bandwidth. *Review of Scientific Instruments* **77**, (2006).
62. Rohrbach,A. Stiffness of optical traps: quantitative agreement between experiment and electromagnetic theory. *Phys. Rev. Lett.* **95**, 168102 (2005).
63. Rohrbach,A., Kress,H. & Stelzer,E.H. Three-dimensional tracking of small spheres in focused laser beams: influence of the detection angular aperture. *Opt. Lett.* **28**, 411-413 (2003).
64. Tischer,C., Pralle,A. & Florin,E.L. Determination and correction of position detection nonlinearity in single particle tracking and three-dimensional scanning probe microscopy. *Microsc. Microanal.* **10**, 425-434 (2004).
65. Rohrbach,A. Switching and measuring a force of 25 femtoNewtons with an optical trap. *Optics Express* **13**, (2005).
66. Sacconi,L., Tolic-Norrelykke,I.M., Stringari,C., Antolini,R. & Pavone,F.S. Optical micromanipulations inside yeast cells. *Appl. Opt.* **44**, 2001-2007 (2005).

67. Desai,K.V. *et al.* Agnostic particle tracking for three-dimensional motion of cellular granules and membrane-tethered bead dynamics. *Biophys. J.* **94**, 2374-2384 (2008).
68. Lukosz,W. & Warga,M.E. Thd11 - A New Theorem on Ultimate Limit of Performance of Optical Systems. *Journal of the Optical Society of America* **56**, 548-& (1966).
69. Alberto Diaspro. Confocal and Two-Photon Microscopy: Foundations, Applications and Advances. (2002).
70. Joseph R.Lakowicz. Principles of Fluorescence Spectroscopy. (2007).
71. Betzig,E. *et al.* Imaging intracellular fluorescent proteins at nanometer resolution. *Science* **313**, 1642-1645 (2006).
72. Periasamy,A., Elangovan,M., Elliott,E. & Brautigan,D.L. Fluorescence lifetime imaging (FLIM) of green fluorescent fusion proteins in living cells. *Methods Mol. Biol.* **183**, 89-100 (2002).
73. Bastiaens,P.I. & Squire,A. Fluorescence lifetime imaging microscopy: spatial resolution of biochemical processes in the cell. *Trends Cell Biol.* **9**, 48-52 (1999).
74. Gauderon,R., Lukins,P.B. & Sheppard,C.J. Three-dimensional second-harmonic generation imaging with femtosecond laser pulses. *Opt. Lett.* **23**, 1209-1211 (1998).
75. Svoboda,K. & Block,S.M. Biological Applications of Optical Forces. *Annual Review of Biophysics and Biomolecular Structure* **23**, 247-285 (1994).
76. Laan,L., Husson,J., Munteanu,E.L., Kerssemakers,J.W. & Dogterom,M. Force-generation and dynamic instability of microtubule bundles. *Proc. Natl. Acad. Sci. U. S. A* **105**, 8920-8925 (2008).
77. Christian Tischer *et al.* Three-dimensional thermal noise imaging. Applied Physics Letters 79(23). 3-12-2001.
78. Neuman,K.C., Chadd,E.H., Liou,G.F., Bergman,K. & Block,S.M. Characterization of photodamage to Escherichia coli in optical traps. *Biophysical Journal* **77**, 2856-2863 (1999).
79. Kurt D.Wulff *et al.* Aberration correction in holographic optical tweezers. *Optics Express* **14**, 4169-4174 (2006).
80. Vicidomini,G., Mondal,P.P. & Diaspro,A. Fuzzy logic and maximum a posteriori-based image restoration for confocal microscopy. *Opt. Lett.* **31**, 3582-3584 (2006).
81. Difato,F. *et al.* Improvement in volume estimation from confocal sections after image deconvolution. *Microsc. Res. Tech.* **64**, 151-155 (2004).
82. Diaspro,A., Corosu,M., Ramoino,P. & Robello,M. Adapting a compact confocal microscope system to a two-photon excitation fluorescence imaging architecture. *Microscopy Research and Technique* **47**, 196-205 (1999).
83. Periasamy,A., Skoglund,P., Noakes,C. & Keller,R. An evaluation of two-photon excitation versus confocal and digital deconvolution fluorescence microscopy imaging in Xenopus morphogenesis. *Microscopy Research and Technique* **47**, 172-181 (1999).
84. Tatarkova,S.A., Sibbett,W. & Dholakia,K. Brownian particle in an optical potential of the washboard type. *Phys. Rev. Lett.* **91**, 038101 (2003).
85. Lukic,B. *et al.* Direct observation of nondiffusive motion of a Brownian particle. *Phys. Rev. Lett.* **95**, 160601 (2005).
86. Egner,A., Andresen,V. & Hell,S.W. Comparison of the axial resolution of practical Nipkow-disk confocal fluorescence microscopy with that of multifocal multiphoton microscopy: theory and experiment. *Journal of Microscopy-Oxford* **206**, 24-32 (2002).
87. Hell,S., Reiner,G., Cremer,C. & Stelzer,E.H.K. Aberrations in Confocal Fluorescence Microscopy Induced by Mismatches in Refractive-Index. *Journal of Microscopy-Oxford* **169**, 391-405 (1993).
88. Booth,M.J. Adaptive optics in microscopy. *Philos. Transact. A Math. Phys. Eng Sci.* **365**, 2829-2843 (2007).
89. Bertero M. & Boccaccio P. Introduction to Inverse Problems in Imaging. (1998).

90. Hiroshi Kano, Hans T M van der Voort, ,M.S., ,G.M.P.v.K. & and Stefan W Hell. Avalanche photodiode detection with object scanning and image restoration provides 2–4 fold resolution increase in two-photon fluorescence microscopy. *bioimaging* **4**, 187-197 (1996).
91. Ericsson,M., Hanstorp,D., Hagberg,P., Enger,J. & Nystrom,T. Sorting out bacterial viability with optical tweezers. *Journal of Bacteriology* **182**, 5551-5555 (2000).
92. Sacconi,L. *et al.* In vivo multiphoton nanosurgery on cortical neurons. *J. Biomed. Opt.* **12**, 050502 (2007).
93. Visscher,K. & Brakenhoff,G.J. Single Beam Optical Trapping Integrated in A Confocal Microscope for Biological Applications. *Cytometry* **12**, 486-491 (1991).
94. Wilson T. & Sheppard C.J.R. Theory and Practice of Scanning. Optical Microscopy. (1984).
95. Meng,F. & Ma,H. Fluorescence correlation spectroscopy analysis of diffusion in a laser gradient field: a numerical approach. *J. Phys. Chem. B* **109**, 5580-5585 (2005).
96. Bustamante,C., Marko,J.F., Siggia,E.D. & Smith,S. Entropic elasticity of lambda-phage DNA. *Science* **265**, 1599-1600 (1994).
97. Lang,M.J., Fordyce,P.M., Engh,A.M., Neuman,K.C. & Block,S.M. Simultaneous, coincident optical trapping and single-molecule fluorescence. *Nature Methods* **1**, (2004).
98. M Capitanio, D Maggi, F Vanzi & F S Pavone. FIONA in the trap: the advantages of combining optical tweezers and fluorescence. *J. Opt. A: Pure Appl. Opt.* **9**, (2007).
99. Yu-Li Wang & Dennis E.Discher. Cell Mechanics. (2007).
100. Cai,Y. *et al.* Nonmuscle myosin IIA-dependent force inhibits cell spreading and drives F-actin flow. *Biophys. J.* **91**, 3907-3920 (2006).
101. Palazzo,A.F., Eng,C.H., Schlaepfer,D.D., Marcantonio,E.E. & Gundersen,G.G. Localized stabilization of microtubules by integrin- and FAK-facilitated Rho signaling. *Science* **303**, 836-839 (2004).
102. Adams,J.C. *et al.* Cell-matrix adhesions differentially regulate fascin phosphorylation. *Molecular Biology of the Cell* **10**, 4177-4190 (1999).
103. Carlsson,A.E. Growth of branched actin networks against obstacles. *Biophysical Journal* **81**, 1907-1923 (2001).
104. Liu,A.P. & Fletcher,D.A. Actin polymerization serves as a membrane domain switch in model lipid bilayers. *Biophysical Journal* **91**, 4064-4070 (2006).
105. Raucher,D. & Sheetz,M.P. Cell spreading and lamellipodial extension rate is regulated by membrane tension. *Journal of Cell Biology* **148**, 127-136 (2000).
106. Dai,J. & Sheetz,M.P. Cell membrane mechanics. *Methods Cell Biol.* **55**, 157-171 (1998).
107. Sheetz,M.P. & Dai,J. Modulation of membrane dynamics and cell motility by membrane tension. *Trends Cell Biol.* **6**, 85-89 (1996).
108. Apodaca,G. Modulation of membrane traffic by mechanical stimuli. *Am. J. Physiol Renal Physiol* **282**, F179-F190 (2002).
109. Hochmuth,R.M., Shao,J.Y., Dai,J.W. & Sheetz,M.P. Deformation and flow of membrane into tethers extracted from neuronal growth cones. *Biophysical Journal* **70**, 358-369 (1996).
110. Mogilner,A. & Oster,G. Polymer motors: Pushing out the front and pulling up the back. *Current Biology* **13**, R721-R733 (2003).
111. Pralle,A. & Florin,E.L. Cellular membranes studied by photonic force microscopy. *Methods Cell Biol.* **68**, 193-212 (2002).
112. Tolic-Norrelykke,I.M., Munteanu,E.L., Thon,G., Oddershede,L. & Berg-Sorensen,K. Anomalous diffusion in living yeast cells. *Phys. Rev. Lett.* **93**, 078102 (2004).
113. Carlier,M.F., Le Clainche,C., Wiesner,S. & Pantaloni,D. Actin-based motility: from molecules to movement. *Bioessays* **25**, 336-345 (2003).

114. Footer,M.J., Kerssemakers,J.W.J., Theriot,J.A. & Dogterom,M. Direct measurement of force generation by actin filament polymerization using an optical trap. *Proceedings of the National Academy of Sciences of the United States of America* **104**, 2181-2186 (2007).
115. Kovar,D.R. & Pollard,T.D. Insertional assembly of actin filament barbed ends in association with formins produces piconewton forces. *Proceedings of the National Academy of Sciences of the United States of America* **101**, 14725-14730 (2004).
116. Shaevitz,J.W. & Fletcher,D.A. Load fluctuations drive actin network growth. *Proc. Natl. Acad. Sci. U. S A* **104**, 15688-15692 (2007).
117. Dent,E.W. & Kalil,K. Axon branching requires interactions between dynamic microtubules and actin filaments. *Journal of Neuroscience* **21**, 9757-9769 (2001).
118. Carlier,M.F.T., Loisel,T.P., Boujemaa,R. & Pantaloni,D. Reconstitution of actin-based motility of Listeria and Shigella using pure proteins. *Biophysical Journal* **78**, 240A (2000).
119. McGrath,J.L. *et al.* The force-velocity relationship for the actin-based motility of Listeria monocytogenes. *Current Biology* **13**, 329-332 (2003).
120. Noireaux,V. *et al.* Growing an actin gel on spherical surfaces. *Biophysical Journal* **78**, 1643-1654 (2000).
121. Cameron,L.A., Svitkina,T.M., Vignjevic,D., Theriot,J.A. & Borisy,G.G. Dendritic organization of actin comet tails. *Current Biology* **11**, 130-135 (2001).
122. Mogilner,A. & Oster,G. Force generation by actin polymerization II: The elastic ratchet and tethered filaments. *Biophysical Journal* **84**, 1591-1605 (2003).
123. Parekh,S.H., Chaudhuri,O., Theriot,J.A. & Fletcher,D.A. Loading history determines the velocity of actin-network growth. *Nat. Cell Biol.* **7**, 1219-1223 (2005).
124. Theriot,J.A. Actin Polymerization and the Propulsion of Listeria-Monocytogenes. *Biophysical Journal* **66**, A352 (1994).
125. Gerbal,F. *et al.* Measurement of the elasticity of the actin tail of Listeria monocytogenes. *European Biophysics Journal with Biophysics Letters* **29**, 134-140 (2000).
126. Theriot,J.A. & Fung,D.C. Listeria monocytogenes-based assays for actin assembly factors. *Methods Enzymol.* **298**, 114-122 (1998).
127. Kress,H. *et al.* Filopodia act as phagocytic tentacles and pull with discrete steps and a load-dependent velocity. *Proc Natl Acad Sci U. S. A* **104**, 11633-11638 (2007).
128. Cojoc,D. *et al.* Properties of the force exerted by filopodia and lamellipodia and the involvement of cytoskeletal components. *PLoS. ONE.* **2**, e1072 (2007).
129. Allioux-Guerin,M. *et al.* Spatio-temporal analysis of cell response to a rigidity gradient: a quantitative study by multiple optical tweezers. *Biophys. J.* (2008).
130. Sheetz,M.P., Sable,J.E. & Dobereiner,H.G. Continuous membrane-cytoskeleton adhesion requires continuous accommodation to lipid and cytoskeleton dynamics. *Annu. Rev. Biophys. Biomol. Struct.* **35**, 417-434 (2006).
131. Ashkin,A. & Dziedzic,J.M. Optical Trapping and Manipulation of Viruses and Bacteria. *Science* **235**, 1517-1520 (1987).
132. Bustamante,C., Macosko,J.C. & Wuite,G.J.L. Grabbing the cat by the tail: Manipulating molecules one by one. *Nature Reviews Molecular Cell Biology* **1**, 130-136 (2000).
133. Jeney,S., Florin,E.L. & Horber,J.K. Use of photonic force microscopy to study single-motor-molecule mechanics. *Methods Mol. Biol.* **164**, 91-108 (2001).
134. Molloy,J.E. & Padgett,M.J. Lights, action: optical tweezers. *Contemporary Physics* **43**, 241-258 (2002).
135. Wang,M.D. *et al.* Force and velocity measured for single molecules of RNA polymerase. *Science* **282**, 902-907 (1998).
136. P.Michael Conn. Laser Capture Microscopy. (2002).

137. Colombelli,J., Reynaud,E.G. & Stelzer,E.H. Investigating relaxation processes in cells and developing organisms: from cell ablation to cytoskeleton nanosurgery. *Methods Cell Biol.* **82**, 267-291 (2007).
138. Stracke,F., Rieman,I. & Konig,K. Optical nanoinjection of macromolecules into vital cells. *J. Photochem. Photobiol. B* **81**, 136-142 (2005).
139. Steubing,R.W., Cheng,S., Wright,W.H., Numajiri,Y. & Berns,M.W. Laser induced cell fusion in combination with optical tweezers: the laser cell fusion trap. *Cytometry* **12**, 505-510 (1991).
140. Schneckenburger,H., Hendinger,A., Sailer,R., Strauss,W.S. & Schmitt,M. Laser-assisted optoporation of single cells. *J. Biomed. Opt.* **7**, 410-416 (2002).
141. Berns,M.W. *et al.* Laser microsurgery in cell and developmental biology. *Science* **213**, 505-513 (1981).